



RESEARCH ARTICLE - ENGINEERING

Numerical Study to Investigate the Performance of U-shaped Flat Plate Solar Collector Using Phase Change Materials (PCMs)

Ibrahim Lazim Ihnayish¹, Ahmed Qasim Ahmed^{1*}, Abdulrahman Th. Mohammad², Ali Khalid Shaker Al-Syab³

¹ Engineering Technical College - Baghdad, Middle Technical University, Baghdad, Iraq

² Technical Institute / Baquba, Middle Technical University, Baghdad, Iraq

³ Department of Mechanical Engineering and Construction, Campus de Riu Sec s/n, Universitat Jaume I, 12071 Castelló de la Plana, Spain

* Corresponding author E-mail: en_ahmed82@yahoo.com

Article Info.	Abstract
<p><i>Article history:</i></p> <p>Received 10 March 2023</p> <p>Accepted 02 May 2023</p> <p>Publishing 30 June 2023</p>	<p>Thermal solar collector considers one of the main devices employed to transform solar energy into thermal energy and can be classified into three main types named Evacuated tube collector (ETC), flat plate collector (FPC), and compound parabolic collector (CPC) collector. In this study, where it was taken to evacuated tube solar collectors three different geometries of the inner pipe diameter were proposed and combined with type of phase change materials (PCM) to evaluate their performance using PCM. And mass flow rate 0.5 L/min, A validated computational fluid dynamic (CFD) model was used in this examination. The data indicates that the highest outlet water temperature was observed at 45 °C from 1:00 pm to 2:00 pm for case-1 with a smooth pipe, whereas for case-2 with two lobes and case-3 with four lobes, the maximum temperatures were 41 °C and 40 °C, respectively, The results showed that case-1 with Paraffin wax has the best efficiency among the proposed cases. Where it was recorded maximum outlet water temperature was about 45 °C.</p>

This is an open-access article under the CC BY 4.0 license (<http://creativecommons.org/licenses/by/4.0/>)

Publisher: Middle Technical University

Keywords: Solar Energy; Solar Collector; CFD; Evacuated Tube; PCM.

1. Introduction

Renewable energy has become a popular source that is contributed to solving the problems of increasing demand for electrical energy. Where it is considered as friendly to the environment. Among the types of renewable energies, solar energy is the main important source that is widely used today. Generally, the energy of the sun can be converted into two useful energies such as electrical energy and thermal energy [1]. Solar energy is transformed into thermal energy by using thermal collectors [2] and stored in some fluids like water or solid materials such as phase change materials (PCMs). Thermal collector plays a big role and a main part in the thermal solar systems that concluded the domestic hot water and commercial solar power systems [3-4]. The main classification of solar collectors can be divided according to the tracker mechanism into non-tracking, one-axis tracking, and two axes tracking. The types of non-tracking collectors can be named as Evacuated tube collector (ETC), flat plate collector (FPC), and compound parabolic collector (CPC) collector. FPC is a simple and most common collector among the kinds of solar collectors. It is used in medium and low-temperature applications [5-7], involving industrial and building heating systems. A number of the ETC designs have been developed. In a simple design, many long cylindrical flat plate modules are installed side-by-side. Each module is a cylindrical evacuated glass tube containing a metal absorber plate in a rectangular form; therefore, many researchers have worked to improve its efficiency using different techniques. Farzad and Abdi 2012 [8] investigated both theoretically and experimentally the capacity of the evacuated solar heat pipe collector. Formulas for heat transmission were employed in the process of theoretical modelled, and a technique tested based on ISO 9806-1 was used so that the theoretical model could be equated to the results of the experiment. Both the theoretical and practical approaches were evaluated regarding the efficiency of the collectors and the amount of usable heat gained. It was shown that the theoretical models matched well with the experimental data and that they were able to properly estimate the performance, temperature, and usable heat gain of an evacuated heat pipe collector of working fluids at the outlet. Riffat et al. 2006 [9] investigated experimentally the effect of using storage energy by PCM on thermal efficiency systems. Five different cases, including a referenced case, were investigated experimentally, and the system performance of each was analyzed and integrated with an evacuated tube collector. Many experiments were made, and the collector gave a better efficiency when filled with 25.28% of water. Zhang and Yamaguchi 2008 [10] used a specially designed stainless-steel U-shaped pipe with a fin to collect energy from the fluid being tested in an evacuated tube.

Nomenclature & Symbols			
PV	photovoltaic	Ti	Inlet water temperature (°C)
PCM	phase change materials	To	Outlet water temperature (°C)
ETC	Evacuated tube collector	G	Solar irradiance (W/m ²)
FPC	Flat plate collector.	mf	Mass fraction
CPC	Compound parabolic collector.	Pmax	Maximum electrical power (W)
CFD	Computational fluid dynamic.	Ts	Surface temperature (°C)

They found that solar radiation affected the different phases of CO₂, including liquid, liquid-gas, and supercritical phases, as well as the mass flow rate of CO₂. This suggests that solar radiation can have a significant impact on the behavior of CO₂ in different phases, which could have important implications for energy collection and storage technologies. Mat et al. 2013 [11] investigated numerically using RT 82 PCM, which dissolves at 77 °C in the system to enhance the performance. Throughout the experiment, the position of the heat source moved a total of 29 times. The results revealed that the introduction of fins significantly improved heat transmission and shortened melting times by 43.3%. Ong and Tong 2013 [12] performed a comparison study between the outdoor efficiency of the two systems of solar water heaters. The result revealed that the installed panel solar collector's system gave the best compared with the vertical panel solar collector's system. Xinyu and Shijun 2014 [13] studied the performance of extraction heat-based direct-flow of coaxial ETSC experimentally with and without heat shields. It was designed to create a tested system to measure the thermal efficiency of solar collectors operated at middle temperatures. The results showed that the heat shield improved the efficiency of an ETSC, particularly at higher temperatures. Dilip Mishra 2015 [14] studied the influence of using the evacuated tube solar collector (ETSC) with a U-tube on system efficiency experimentally. The results revealed that the idea of the inserted copper fin into it increase the system performance of the ETSC from 10% to 15% from the water-in-glass evacuated collector. Yao et al. 2015 [15] examined the impact of twisted inserts on the performance of the evacuated tube for solar water heaters. Twisted tape reduces velocity magnitude and maintains temperature uniformity. The results revealed the improved solar water heaters were 9.29% higher than the regular ones. Abokersh et al. 2017 [16] Studied experimentally the possibility of applying the PCM in a similar method where the added aluminum fins were on the U-shape tube outer surface and the tube inner surface for the glass absorber. The result showed that adding the aluminum fins improve the heat retention capacity and decreasing in thermal performance by 14% compared to that of the design using only the PCM and without the aluminum fins. Feliński and Sekret 2017 [17] studied, in a controlled experiment, the influence of paraffin application on the performance of the evacuated tube solar collector and storage (ETC/S) system. Based on the heated medium mass flow rate during the discharge period, the findings demonstrated that the total quantity of heat produced from paraffin integrated ETC/S system was enhanced by up to 45-79% compared with an ETC. Although the reviewed papers provide valuable insights into improving the efficiency of solar collectors and storage systems, some limitations need to be addressed. Firstly, most of the studies are focused on experimental and numerical analysis, which may not necessarily reflect real-life conditions. Secondly, the studies mainly focus on the performance of specific types of solar collectors and do not compare their effectiveness with other types of solar collectors. Finally, some studies lack detailed information on the cost-effectiveness and scalability of the proposed designs.

To overcome these limitations, this work proposes a comprehensive review that considers different types of solar collectors and their performance in real-life conditions. The review will also assess the cost-effectiveness and scalability of the proposed designs, making it easier for researchers and policymakers to determine the most effective and feasible approach for implementing solar collectors and storage systems. Additionally, the review will analyze both experimental and numerical studies to provide a more comprehensive understanding of the performance of solar collectors and storage systems. Overall, this work aims to provide a more holistic and practical approach to improving the efficiency of solar collectors and storage systems. where especially this theoretical study focuses on the change in U-shaped pipes. smooth pipe, two lobes, and four lobes.

2. Methods

Computational Fluid Dynamics (CFD) has become an important method to evaluate and solve many engineering problems such as the behavior of phase change materials (PCMs) in the evacuated tube. For such a problem, detailed information on temperature distribution and flow can be obtained by using a CFD method. In addition, choosing a suitable CFD model can provide an accurate simulating result at a low cost compared with the experimental part. Therefore, in this study, a CFD model using ANSYS Fluent was employed to investigate and obtain more details of the influence of using (PCMs) in different geometry of the evacuated tube. To obtain an accurate prediction in the CFD model, many points need to be taken carefully such as type of (PCMs), tube dimension, radiation, and flow rate. In addition, selecting an appropriate CFD model consider one of the main important factors in simulation results. The correct CFD model will help to get a stable simulation process and give accurate simulation results. This was obtained by solving the partial differential equations of continuity, energy equations, and momentum.

The Navier-Stokes equations with phase change materials, also known as the phase change Navier-Stokes equations, are a set of partial differential equations that describe the motion of fluids and the phase change process.

The equations are based on the conservation of mass, momentum, and energy, and are given by:

Conservation of mass:

$$\partial\rho/\partial t + \nabla \cdot (\rho \mathbf{u}) = 0$$

where ρ is the fluid density, t is time, \mathbf{u} is the fluid velocity and ∇ is the gradient operator.

Conservation of momentum:

$$\rho (\partial\mathbf{u}/\partial t + \mathbf{u} \cdot \nabla\mathbf{u}) = -\nabla P + \nabla \cdot \boldsymbol{\tau}$$

where P is the pressure, and $\boldsymbol{\tau}$ is the stress tensor, given by:

$$\boldsymbol{\tau} = \mu (\nabla\mathbf{u} + (\nabla\mathbf{u})^T) - \kappa \nabla T$$

where μ is the dynamic viscosity, T is the temperature, κ is the thermal conductivity, and $(\nabla\mathbf{u})^T$ is the transpose of the gradient of \mathbf{u} .

Conservation of energy:

$$\rho c_p (\partial T/\partial t + \mathbf{u} \cdot \nabla T) = \nabla \cdot (\kappa \nabla T) + Q$$

where c_p is the specific heat capacity at constant pressure, and Q is the heat source term due to phase change.

In addition to the above equations, the phase change Navier-Stokes equations also include a phase change model that describes the change of phase from one state to another. The phase change model can be added as a source term in the energy equation.

2.1. Investigated case study description

In this investigation, three different geometries of the ETC combined with (PCMs) are examined numerically to find the influence of using the (PCMs) on ETC performance at three different geometries. In this study, three cases, case-(1), case-(2), and case-(3), were simulated at the inner diameter of a glass tube (3.7 cm), and PCM (Paraffin wax 54-57 °C) and different configurations of the inner diameter of copper tube. Where case-1 represents smooth pipe, case-2 represents two lobes pipe and case-3 represents four lobes pipe. Fig. 1 shows the geometry of the present investigated cases. And details of PCMs and the properties of thermophysical of PCMs that were used in the numerical analysis are summarized in Table 1.

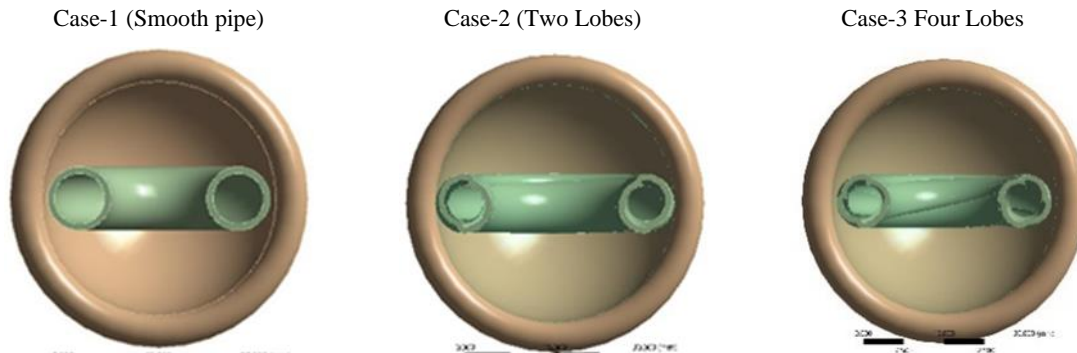


Fig. 1. Geometry of cases under study

Table 1. Thermo-physical properties of PCMs [19]

Properties	Paraffin Wax
Melting Temperature (°C)	54-57
Thermal Conductivity [W/m K]	0.21
The heat of fusion [KJ/Kg]	189
Density [Kg/m ³]	795
Specific heat [kJ/kg K]	2/2.15
Dynamic viscosity of liquid paraffin [kg/m s]	0.023
The thermal expansion coefficient of paraffin [1/K]	0.0003085

2.2. Mesh generation

For any CFD simulation, it is very important to generate a suitable mesh with high quality. This will improve the simulation solution stability and give accurate results. Therefore, in this study, a high-quality mesh with a suitable size was employed. As a complexity of the investigated geometry, as presented in Fig. 2, the ETC geometry was divided into two different zones as shown in Fig. 2. Both types of tetrahedral and hexahedral meshes were utilized to generate the mesh for such complex geometry. About 1,500,000 cells were used in this study. The mesh density was distributed depending on the interesting zone. Where high-density mesh was generated in the area near the walls and (PCMs). Fig. 3 a and b illustrate the mesh distribution for the examined geometry at different views. Fig. 3 c shows detailed information on the mesh used in this study.

2.3. Numerical schemes

In the ANSYS FLUENT software, a pressure-based solver was employed and the PISO scheme with PRESTO mode was employed in this investigation. The square cell base was employed to calculate for gradient using a second-order mode which was employed to calculate the energy and momentum. The convergence of calculations was set at 10^6 for momentum and continuity while for energy equations, the convergence was set to be 10^5 . Momentum, pressure, and liquid fraction were under-relaxed by factors of 0.5, 0.3, and 0.9 respectively. The calculations were performed for 12 hours with a time step of 60 sec. In this investigation, the 3-D model was used for the evacuated U-shape tube with PCMs to calculate the impact of employing the PCMs on ETC performance at different geometry.

2.4. Solar Radiation Simulation

Traditionally, solar collectors were operated using the average solar radiation as a constant heat source [20-21]. However, in this current investigation, unsteady radiation is used to account for the actual amount of solar radiation during each hour experimentally from 8:00 am to 18:00 pm by using a solar meter, which reduces deviations from reality. Fig. 4 shows the solar radiation in Iraq-Baghdad on March 20th, 2022, with the maximum solar radiation occurring at 1:00 PM, which was 950 W/m², gradually decreasing until sunset. The equation below is derived from Fig. 4, which simulates the change of the solar radiation using a User Defined Function (UDF) via MATLAB software program, and import to the Ansys Fluent R19.3 software. Taking into account both the time "t" and amount of solar radiation "G." It is assumed that the reflector applied to the collector produces a uniform G(t) on the outer wall.

$$G(t) = -18.36 t^2 + 160.8 t + 415.84$$

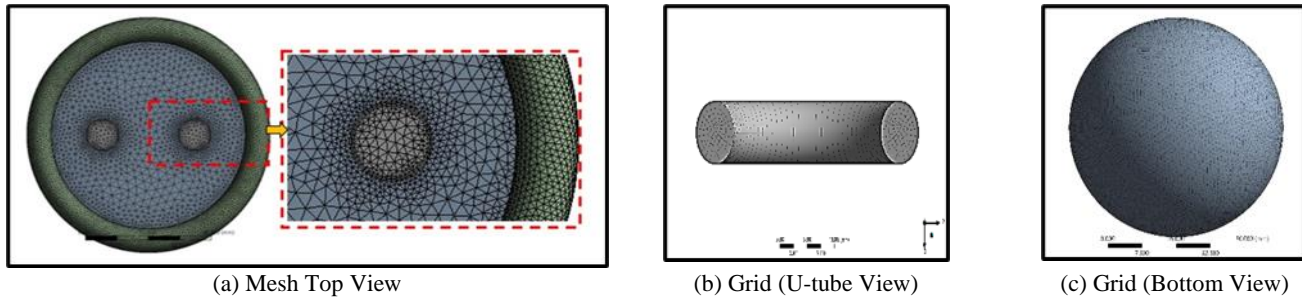


Fig. 2. Grid design for the top and bottom of U-tube of ETC

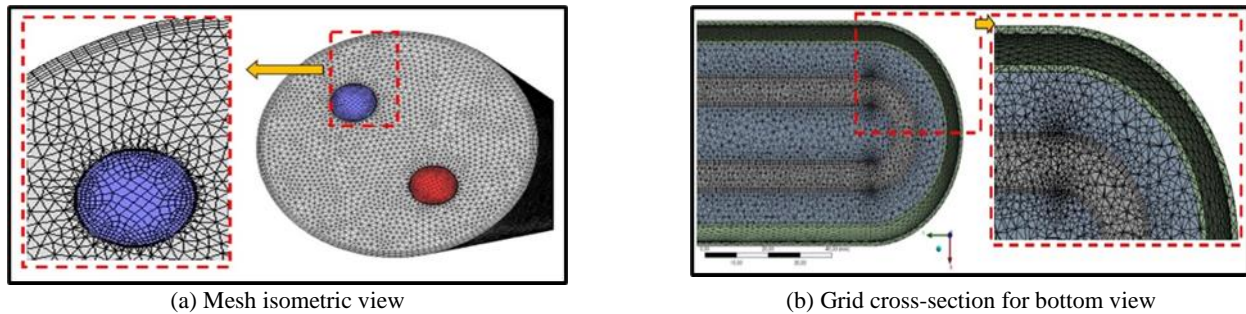


Fig. 3. Grid design for an isometric and cross-section of a U-tube of ETC

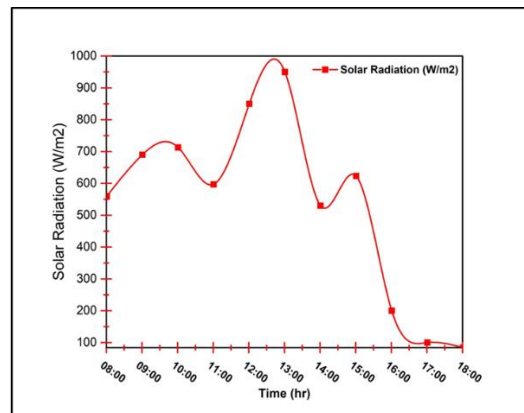


Fig. 4. The profile of solar radiation

3. Validation of Numerical Study

To validate the present numerical model, present simulation results were calculated and compared with an experimental for the previous work Mat [18]. Fig. 5 shows the temperature profile for the previous experimental results and presents numerical results. It is clear to see that the curves in both studies were approximately matching. This gave a good indication of the accuracy of the numerical results.

4. Results and Discussion

4.1. Impact the configuration of the copper tube at 3.7 cm inner diameter of the glass tube and PCM 54-57 °C

The first three cases, case-(1), case-(2), and case-(3), were simulated at the inner diameter of a glass tube (3.7 cm), PCM (Paraffin wax 54-57 °C) and different configurations of the inner diameter of copper tube. Where case-1 represents smooth pipe, case-2 represents two lobes pipe and case-3 represents four lobes pipe. Table 2 presents the contours of the liquid fraction of the three cases from 60 to 720 min. The complete melting was achieved after 180 minutes and the melting rate at the upper plane was higher than the lower one. This was mainly because the force of the natural convection draws the liquid of PCM to the upper section and the solidified PCM sink downward. Moreover, it was noticed that the solid PCM layer around the U-shape copper pipes propagates as an almost similar circular segment surrounding both sides of the copper U-shape. During the period of the charging process from 60 to 480 min, the smooth pipe has a higher melting rate than the two and four lobes. Among the studied smooth pipe, it is showing the smallest melting rate, although the differences between the geometrical pipes were not as marked.

Fig. 6 shows the change in the PCM temperature under the impact of variation of copper tube configuration. It is easy to see that the outlet temperature of PCM with lobes pipes (two and four) is equal to and higher than the PCM temperature with the smooth pipe. In addition, the peak of the outlet temperature was recorded at 79 °C from 1:00 pm until 2:00 pm. Consequently, the lowest temperature of the PCMs was recorded from 4:00 pm until 6:00 pm. This was because that the decrease in the solar radiation and the heat transfer between PCMs and water.

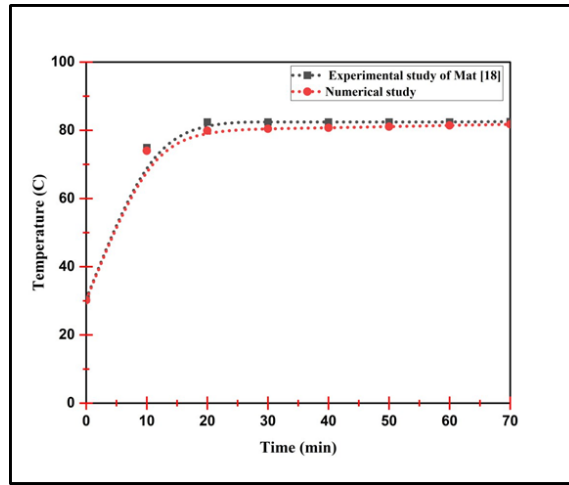


Fig. 5. Comparison study between the previous experimental and present numerical results of the PCM

Table 2. 2D Contours of the liquid fraction at different inner copper tube configurations with an inner diameter of glass tube (3.7) cm and PCM (54-57) °C

Time (min)	Case-1 Glass tube diameter = 3.7 cm and Paraffin wax 54-57 °C	Case -2 Glass tube diameter = 3.7 cm and Paraffin wax 54-57 °C	Case -3 Glass tube diameter = 3.7 cm and Paraffin wax 54-57 °C
60			
300			
600			
720			

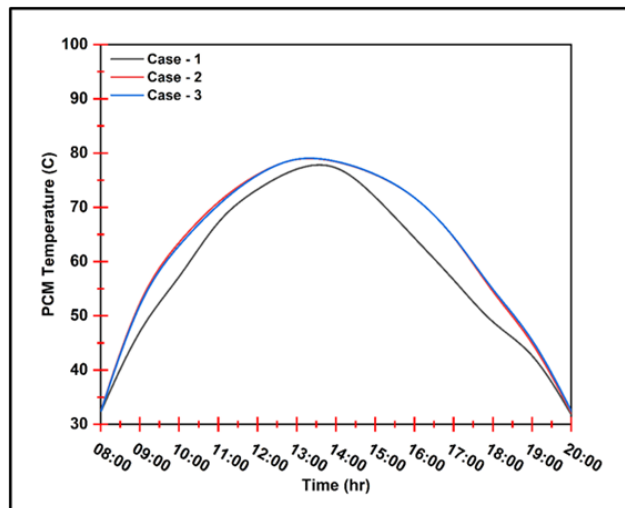


Fig. 6. Average PCM temperature for the three cases-1,2,3

Fig. 8 displays the variations in outlet water temperature for cases-1, 2, and 3. It is clear that the maximum outlet water temperature was recorded at 45 °C between 1:00 pm to 2:00 pm for case-1 while, it was recorded at 41 °C and 40 °C in case-2 and case-3 respectively.

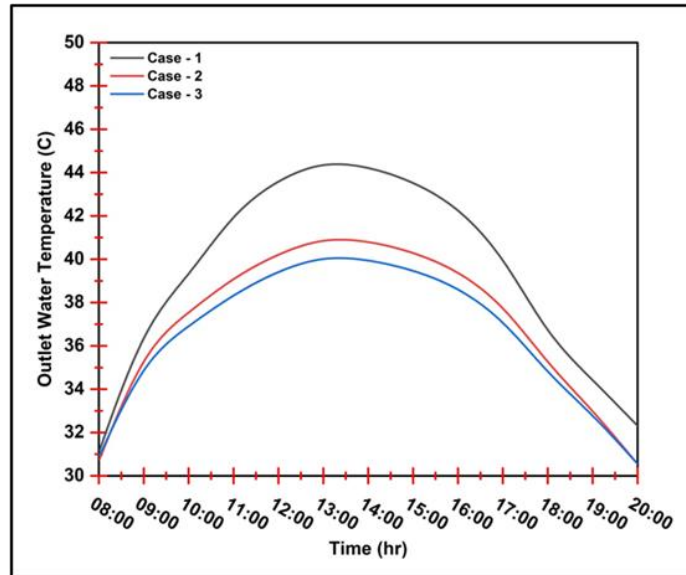


Fig. 8. Displays the variations of the PCM liquid fraction for the three cases

As shown in Fig. 9, the PCM liquid fraction of case-1 was recorded at a high level of about 0.94 in case-1 at the melting point at 1:00 pm while it was recorded at about the same value in case-2 and case-3. The PCM can fully melt and this continues when solar radiation is high at noon, and this is called charging and then started decreasing in liquid fraction this is called as discharging process and this was due to decrease the solar radiation where the PCMs send the stored heat to the working heat fluid.

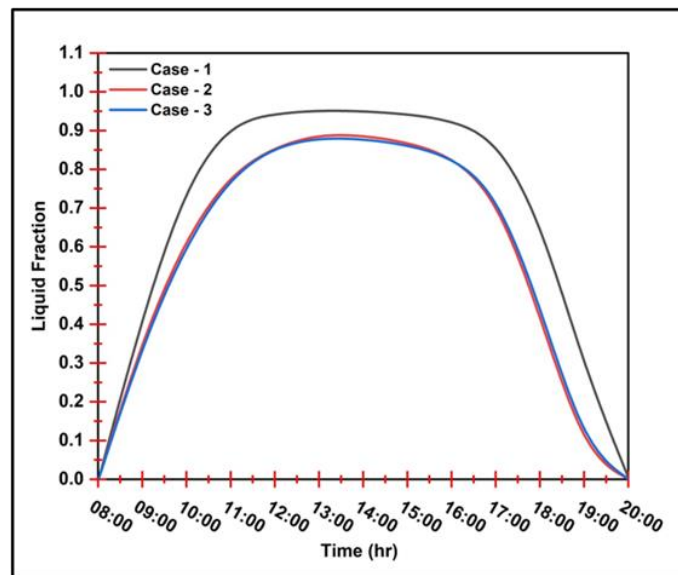


Fig. 9. Liquid fraction charging and discharging process for three cases-1, 2, and 3

5. Conclusion

The objective of this paper was to analyse the effect of three different geometry, smooth, two-lobed, and four-lobed pipes, on the thermal performance of the ETSC that is filled by PCM. This investigation employed a numerical simulation for the melting and solidification phases and assessed the impact of the number of lobes, depth corrugated, and pitch on various performance metrics. The findings are presented below.

- The phase change process commenced at 9:00 AM and persisted until 15:00 PM to ensure the collector was fully charged. During this period, the melting process was also underway, and by 13:30 PM, the heat working fluid had attained the desired outlet temperature of 45°C, rendering the system suitable for domestic hot water applications.
- During the charging process, when the number of lobes was examined, the rate of change in the outlet temperature and liquid fraction was not substantially different between the smooth pipe, two-lobe, and four-lobe pipes. Consequently, the corrugated tube was found to be ineffective during the melting process.
- When examining the number of lobes during the discharging process, it was discovered that the smooth pipe could sustain the operational temperature of the collector until 20:00 PM, up to a maximum of 36 °C.

Acknowledgements

The authors would like to thank the Middle Technical University for the financial support of this project.

References

- [1] H. Li, H. Lin, Q. Tan, P. Wu, C. Wang, G. De, and L. Huang., "Research on the policy route of China's distributed photovoltaic power generation," *Energy Reports*, vol. 6, pp. 254–263, 2020. <https://doi.org/10.1016/j.egy.2019.12.027>.
- [2] M. Dannemand, B. Perers, and S. Furbo. "Performance of a demonstration solar PVT assisted heat pump system with cold buffer storage and domestic hot water storage tanks," *Energy Build.*, vol. 188, pp. 46–57, 2019. <https://doi.org/10.1016/j.enbuild.2018.12.042>.
- [3] K. A. Moharram, M. S. Abd-Elhady, H. A. Kandil, and H. El-Sherif, "Enhancing the performance of photovoltaic panels by water cooling," *Ain Shams Eng. J.*, vol. 4, no. 4, pp. 869–877, 2013. <http://dx.doi.org/10.1016/j.asej.2013.03.005>.
- [4] S. Suman, M. K. Khan, and M. Pathak, "Performance enhancement of solar collectors - A review," *Renew. Sustain. Energy Rev.*, vol. 49, pp. 192–210, 2015, doi: 10.1016/j.rser.2015.04.087. <http://dx.doi.org/10.1016/j.rser.2015.04.087>.
- [5] Y. Liu, C. Tan, Y. Jin, and S. Ma, "Heat collection performance analysis of corrugated flat plate collector: An experimental study," *Renew. Energy*, vol. 181, pp. 1–9, 2022. <https://doi.org/10.1016/j.renene.2021.09.001>.
- [6] R. Dobriyal, P. Negi, N. Sengar, and D. B. Singh, "A brief review on solar flat plate collector by incorporating the effect of nanofluid," *Mater. today Proc.*, vol. 21, pp. 1653–1658, 2020. <https://doi.org/10.1016/j.matpr.2019.11.294>.
- [7] S. Kalogirou, "The potential of solar industrial process heat applications," *Appl. Energy*, vol. 76, no. 4, pp. 337–361, 2003. [https://doi.org/10.1016/S0306-2619\(02\)00176-9](https://doi.org/10.1016/S0306-2619(02)00176-9).
- [8] F. Jafarkazemi, and H. Abdi, "Evacuated tube solar heat pipe collector model and associated tests," *J. Renew. Sustain. Energy*, vol. 4, no. 2, 2012, doi: 10.1063/1.3690958.
- [9] S. Riffat, L. Jiang, J. Zhu, and G. Gan, "Experimental investigation of energy storage for an evacuated solar collector," *Int. J. Low-Carbon Technol.*, vol. 1, no. 2, pp. 139–148, Apr. 2006, doi: 10.1093/ijlct/1.2.139.
- [10] X. R. Zhang, and H. Yamaguchi, "An experimental study on evacuated tube solar collector using supercritical CO₂," *Appl. Therm. Eng.*, vol. 28, no. 10, pp. 1225–1233, 2008, doi: <https://doi.org/10.1016/j.applthermaleng.2007.07.013>.
- [11] A. A. Mat, S. Al-Abidi, A. T. Sopian, K. Sulaiman, and M. Y. Mohammad, "Enhance heat transfer for PCM melting in triplex tube with internal–external fins," *Energy Convers. Manag.*, vol. 74, pp. 223–236, 2013, doi: <https://doi.org/10.1016/j.enconman.2013.05.003>.
- [12] J. K. Ong, K. S. Tong, and W. L. Choong, "Performance of U-tube solar water heater with vertical and inclined panels," *Int. J. Low-Carbon Technol.*, vol. 11, no. 2, pp. 248–253, May 2016, doi: 10.1093/ijlct/ct063.
- [13] S. Zhang, X. You, Y. Ge, H. Gao, and X. Xu, W. Wang, M. He, and T. Zheng, "Thermal performance of direct-flow coaxial evacuated-tube solar collectors with and without a heat shield," *Energy Convers. Manag.*, vol. 84, pp. 80–87, 2014, doi: <https://doi.org/10.1016/j.enconman.2014.04.014>.
- [14] Dilip. Mishra, "Experimental Analysis of Thermal Performance of Evacuated U-Tube Solar Collector," *Advance Physics Letter*. Vol-2, Issue- 3, 2349-1108, pp. 1–7, 2015. 3.5: 12627-12635.
- [15] K. Yao, K. Li, T. Tao, H. Wei, and J. Feng, "Performance Evaluation of All-glass Evacuated Tube Solar Water Heater with Twist Tape Inserts Using CFD," *Energy Procedia*, vol. 70, pp. 332–339, 2015, doi: <https://doi.org/10.1016/j.egypro.2015.02.131>.
- [16] M. H. Abokersh and W. El-Morsi, M. Sharaf, and O. Abdelrahman, "An experimental evaluation of direct flow evacuated tube solar collector integrated with phase change material," *Energy*, vol. 139, pp. 1111–1125, 2017, doi: <https://doi.org/10.1016/j.energy.2017.08.034>.
- [17] R. Feliński, and P. Sekret, "Effect of a low-cost parabolic reflector on the charging efficiency of an evacuated tube collector/storage system with a PCM," *Sol. Energy*, vol. 144, pp. 758–766, 2017. <http://dx.doi.org/10.1016/j.solener.2017.01.073>.
- [18] A. A. Mat, S. Al-Abidi, M. Y. Sopian, K. Sulaiman, and A. T. Mohammad, "Enhance heat transfer for PCM melting in triplex tube with internal–external fins," *Energy Convers. Manag.*, vol. 74, pp. 223–236, 2013, doi: <https://doi.org/10.1016/j.enconman.2013.05.003>.
- [19] M. Olfian, H. Ajarostaghi, S. Farhadi and A. Ramiar, "Melting and solidification processes of phase change material in evacuated tube solar collector with U-shaped spirally corrugated tube," *Appl. Therm. Eng.*, vol. 182, p. 116149, 2021, doi: <https://doi.org/10.1016/j.applthermaleng.2020.116149>.
- [20] C. Korres, and D. Tzivaniadis, "A new mini-CPC with a U-type evacuated tube under thermal and optical investigation," *Renew. Energy*, vol. 128, pp. 529–540, 2018, doi: <https://doi.org/10.1016/j.renene.2017.06.054>.
- [21] R. Ma, L. Lu, Z. Zhang, and J. Liang, "Thermal performance analysis of the glass evacuated tube solar collector with U-tube," *Build. Environ.*, vol. 45, no. 9, pp. 1959–1967, 2010, doi: 10.1016/j.buildenv.2010.01.015.